Research Project and Seminar

Informatik-Ingenieurwesen

Orthogonal Codes for Acoustic UnderwaterLocalization

by

Sergej Keller

April 2022

Supervised by

Christoph Weyer
Institute of Telematics, Hamburg University of Technology

First Examiner | Prof. Dr.-Ing. Bernd-Christian Renner
Institute of Autonomous Cyber-Physical Systems
Hamburg University of Technology

Second Examiner | Prof. Dr. Volker Turau
Institute of Telematics
Hamburg University of Technology

Institute of Autonomous Cyber-Physical Systems
Hamburg University of Technology

TUHH

Acknowledgment

Abstract

Table of Contents

TABLE OF CONTENTS

List of Symbols

$\mathbb{N}, \mathbb{Z}, \mathbb{Q}, \mathbb{R}, \mathbb{C}$	Regular sets of numbers
$\mathcal{NP}, \mathcal{P}$	Complexity classes
$\mathcal{V} = \{v_0, \dots, v_{N-1}\}$	Set of N nodes v_i belonging to a network with sink v_0
ϱ	Node density, i.e., the average number of nodes within another node's communication range
$(v_i, v_j) \in \mathcal{E}$	Set of bidirectional communication links in the network
$G = (\mathcal{V}, \mathcal{E})$	Graph representation of a wireless sensor network
$\mathcal{N}_i = \{v_j \in \mathcal{V} \mid i \neq j \wedge (v_i, v_j) \in \mathcal{E}\}$	The set of bidirectional communication partners of node v_i
$\mathcal{T} \subseteq \mathcal{E}, \quad \lvert\mathcal{T}\rvert = N-1$	Routing tree rooted in the sink
$\mathcal{T}_i$	Subtree rooted in (and including) node v_i
$\mathcal{C}_i, \quad C_i = \lvert\mathcal{C}_i\rvert$	The set and number of children of node v_i in $\mathcal{T}$
$\mathcal{F} = \{v_i \in \mathcal{V} \mid \mathcal{C}_i = \emptyset\}$	Set of leafs in $\mathcal{T}$ and the number of leafs
$\mathcal{F}_i$	Set of leafs in the subtree $\mathcal{T}_i$ of $\mathcal{T}$

List of Symbols

Chapter 1

Introduction

Acoustic signals are nowadays mostly used for military and research propose. Electromagnetic waves cant perpetuate water, so by the use of acoustic modems water can be used as a medium. Underwater vehicles need to be capable of communicate to either themselves or objects placed at the surface. Even though the throughput of these acoustic signals is way less than its electromagnetic counterpart, it still has the advantage to perpetuate fluids.

1.1 Motivation

Using water as a medium for localization signals can be somewhat sophisticated to implement and are therefore a challenging research topic. Due strong damping of the classic electromagnetic waves general technologies like GPS or GLONAS are not applicable in under water scenarios.

Acoustic transmission comes in handy in this case. Most systems use a vehicle which transmits acoustic beacons. These are then received by hydrophones placed at the surface. By estimating the travel times the distance between hydrophones and the underwater vehicle can be calculated. However, to let it localize itself, the reverse method is needed. Thus, anchors firmly fixed at the surface send their individual signals and the vehicle receives them.

Signals send by the anchors need to be separable but still observable. Therefore we need codes that are orthogonal towards each other but nonetheless posses clear auto-correlation.

This project dives into the mathematical details of pseudo.random maximum length sequence generation and signal processing. By the use of cross-correlation and auto-correlation the separation of signals can be implemented and evaluated. USB-Oscilloscope

1.2 Setup

The initial Setup is made of two acoustic anchors placed at a footbridge. An acoustic receiver connected to a USB-Oscilloscope is placed between them.

The advanced setup consists of 4 Anchors fixed at the surface broadcasting different signals produced from an python program. Acoustic Modems use broadcast the transfer band signal into the water. At the beginning these 4 anchors need to be synchronized. A blueROV2 receives these signals under water and saves them. Afterward the saved signals are used in python to calculate the position of the ROV.

Figure 1.1: BlueROV2 from Blue Robotics Inc

1.3 Principle

To get the appropriate signals we need to apply certain signal processing steps. First the pseudo-random codes gets up-sampled and put though an cosine FIR filter to remove high frequencies from the base-band. The resulting signal is than shifted to the transfer band. Hereon either a custom delay is artificially added by zero padding for the simulation or is send by the acoustic modem.

Because of the advantageous properties of the used codes the different codes can be separated by cross-correlation by the not delayed versions. The cleaner the auto-correlation the higher are the peaks which are used to measure the initial delay. Method of peak detection may needed to filter out peaks caused from reflections.

Chapter 2

PN and orthogonal sequences

There are two main goals need to be pursued for receiving higher localization accuracy.

First the code which is used for the under water localization needs an auto-correlation approaching a Dirac impulse. Resulting in advantageous detection by correlation capabilities.

The next factor are cross-correlation properties, which should meet certain criteria for improving the separation from other sequences. Mathematically speaking, the codes need to be orthogonal to each other or at least approaching orthogonality. These will come in handy if noise, reflections and other artifacts emerge in real world scenarios.

2.1 Pseudo-random codes

There are a couple of techniques to generate PN sequences. Most of these methods use linear feedback shift registers to generate the codes by an initial condition or seed value. In this project I will concertize my research on gold codes, kasami codes and the basic m-sequences which are used for generating gold codes. These types are all based on linear shift registers.

M-sequences are defined as binary PN codes, which are generated by linear shift registers with feedback. The sequences are periodic, and contain an equal number of zeros and ones [PS08]. Maximum length sequences need to fulfill certain criteria. First its length is defined by $N = 2^n - 1$ where n is the maximum degree of the generator polynomial $f(X)$ [SP80].

$$|u| = 2^n - 1 = N, \quad \text{from polynomial } \; h(x) \text{of degree } \; n \tag{2.1}$$

$$\frac{N}{gcd(N,q) = N'}, \quad \text{from decimation polynomials } \; \widetilde{h(x)} \tag{2.2}$$

Second the cross-correlation between m-sequences must take three values only, which are -1, $-t(n)$, $t(n) - 2$. With it $t(n)$ is defined by $1 + 2^{\lfloor 0.5(n+2) \rfloor}$ [SP80]. If every pair of m-sequences is a preferred pair, they form a maximal connected set and these sets have a limited carnality. Experiments from Gold and Koptizke showed that the number of such connected pairs is limited. Between degrees

[GK65]. To get an m-sequence we need a primitive polynomial.

2.1.1 Gold Codes

Because of not optimal cross-correlation properties m-sequences alone are not applicable for the project. But if these type of codes are combined their correlation qualities can change. Gold Codes are m-sequences where two of them with same length are modulo-2 summed. [PS08]

Recent research shows that some gold codes have high similarity to a Gaussian random variable [MD].

$$Gold(u, v) = \{u, v, u \oplus v, u \oplus (v \ll 1), \ldots, u \oplus (v \ll N-1)\} \tag{2.3}$$

2.1.2 Kasami Codes

Kasami sequences are constructed in the similar fashion by using m-sequences with the exception that a second sequence, which is used in the modulo sum, is formed by decimating the default m-sequence by $2^{m/2}$ [PS08] [SP80] [PPWW72]. Thus, only one generator polynomial is required.

$$w = u[2^{N/2}+1] = \{u_1, \ldots, u_i, \ldots, u_N | \text{take every } i\text{-th bit of u}\} \tag{2.4}$$

$$Kasami(u) = \{u, u \oplus w, u \oplus (w \ll 1), \ldots, u \oplus (w \ll 2^{N/2}-2)\} \tag{2.5}$$

2.2 Comparison

For the localization process by orthogonal codes certain criteria needs to be met, which were named in the first chapter. To compare the before explained code types three measures are introduced.

The first one is the peak to side-lobe ratio (PSR) 2.6. This measure is defined by subtracting the mean from the peak of the auto-correlation. Then this value get divided by the standard deviation of the same auto-correlation. A higher PSR value signifies a lower error between the auto correlation and the perfect Dirac resulting in better detection capability. The second one is the ratio between the auto-correlation peak and the maximum of the cross-correlation (ACR) 2.7. There a higher value indicates good code separation qualities.

The comparison is done by sampling pairs at degrees six to ten N times from the set of random sequences. These pairs are then used for generating the wanted pseudo-random codes like gold or kasami. Afterwards for all three code types the shown measures are applied.

$$PSR = \frac{max\{x_{ac}\} - \overline{x_{ac}}}{\sigma_{ac}} \tag{2.6}$$

$$ACR = \frac{max\{x_{ac}\}}{max\{x_{cc}\}} \tag{2.7}$$

From preferred polynomial all possible maximum length sequences, gold sequences and kasami sequences are generated. Then both measures are applied on the cross-correlation and auto-correlation functions of the random codes. The PSR and ACR measures are plotted against the used polynomials. Also the best case of PSR and ACR are plotted by their given correlation function.

Maximum length sequences hold the best auto-correlation properties in comparison to its competitors. But it shows peaks in its cross-correlation, making it a rather bad option for orthogonal separation. The kasami sequence has a way better cross-correlation but still a small peak. The clear winner are gold codes because of the good auto-correlation and very good cross-correlation properties 2.4. Its auto-correlations lags a bit behind its competitors but orthogonality is as much as important.

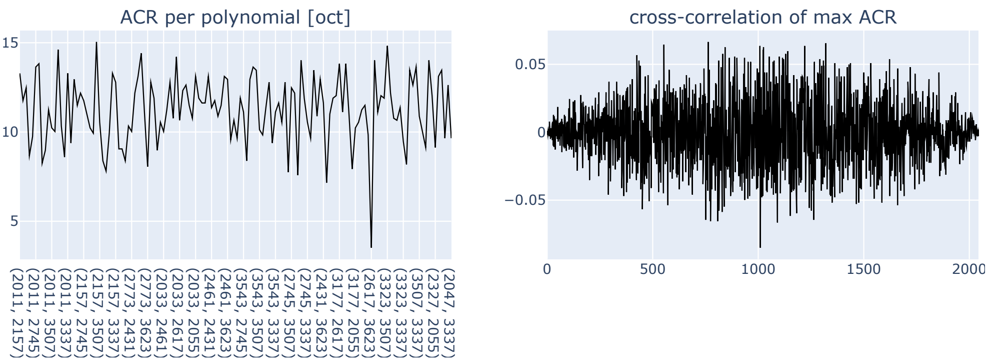

Figure 2.1: Evaluation of gold sequences by AC ratio

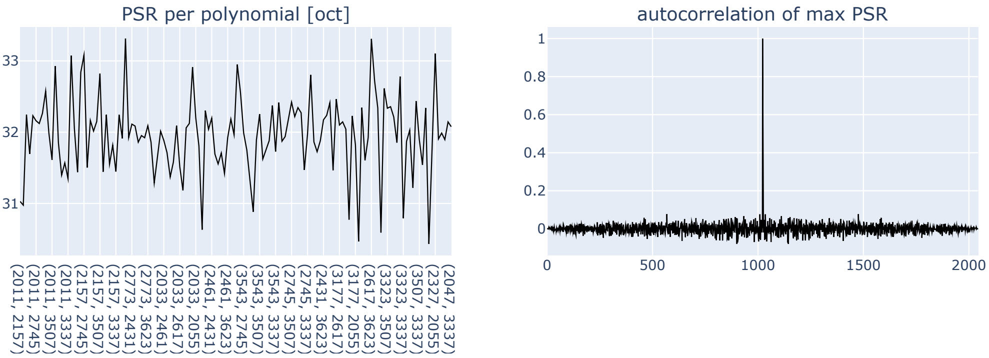

Figure 2.2: Evaluation of gold sequences by PS ratio

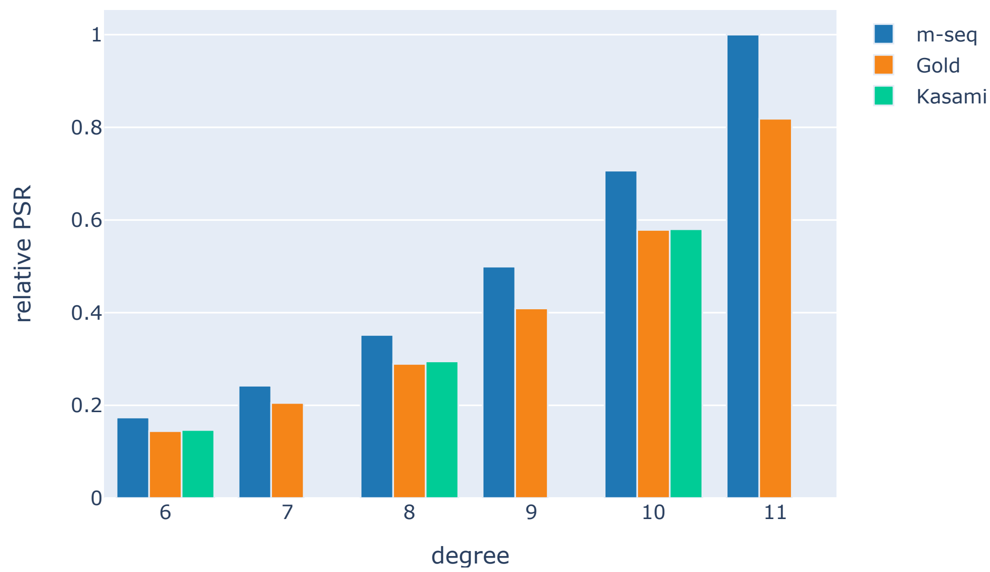

Figure 2.3: Evaluation by relative PSR for degrees 6 to 11

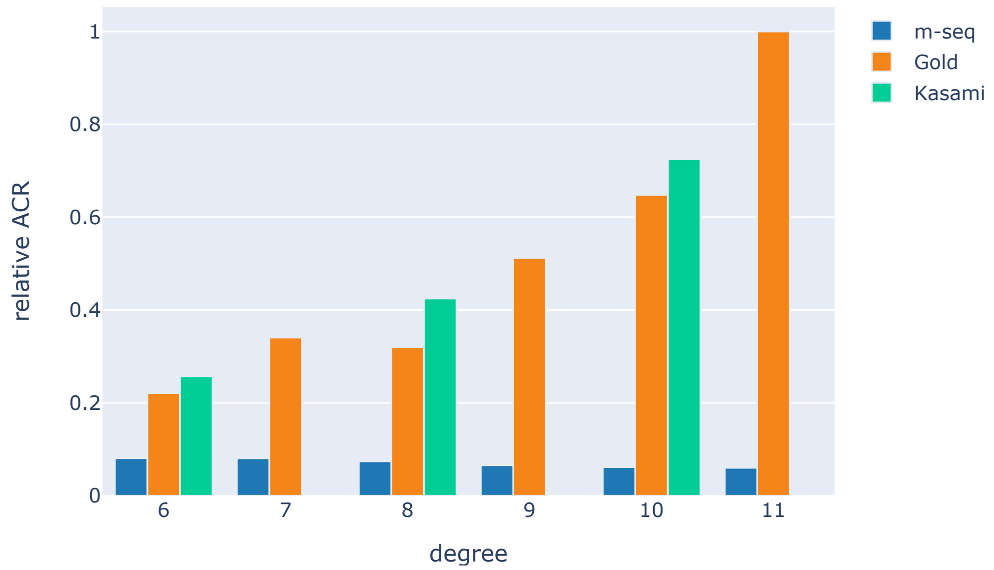

Figure 2.4: Evaluation by relative ACR for degrees 6 to 11

Chapter 3

Signal Processing

After code generation the binary data needs to be transormed into a transmittable signed signal

3.1 Pulse shaping

The raw code which was previously generated is first put through an sign function, which sets its mean to zero. The discontinuous signal holds an infinite bandwidth because it consists of rectangular pulses. These pulse spans have infinity frequency, which are impossible to implement for acoustic transmission. Therefore a restriction to a certain bandwidth must be introduced. Such a reduction is possible by applying an low-pass filter.

Because limiting the signals bandwidth introduces a damped oscillation, which leads to incorrect decoding of received data [Gen07], a appropriate choice of filter would be a the raised cosine 3.1. Such a pulse filter is defined by a squared cosine, which decreases its amplitude in frequency. In our case the roll off factor α is set to 0.125 and symbol length T_{sym} to the inverse of our target bandwidth $20\,kHz$.

Before applying the filter the generated codes need to be up-scaled for our target sampling rate. The relation between sampling rate f_s and up-sampling factor Sp_s is $Sp_s = fs \cdot T_{sym}$.

$$H(\omega) = T_{sym} \cdot \cos^2\left(\frac{T_{sym}(\omega - \pi(1-\alpha)/T_{sym})}{4\alpha}\right), \quad \omega = 2\pi f \tag{3.1}$$

3.2 Shift to Carrier

Now that our base band signal $tSigBB[k]$ has its target bandwidth and sample rate only the frequency shift to the carrier frequency f_c of $62.5\,kHz$ is necessary. That procedure is accomplished by multiplying our sampled signal by the exponential function, where f_c is passed to its exponent. The resulting signal could hold imaginary parts, hence only the real part is passed through for transmission.

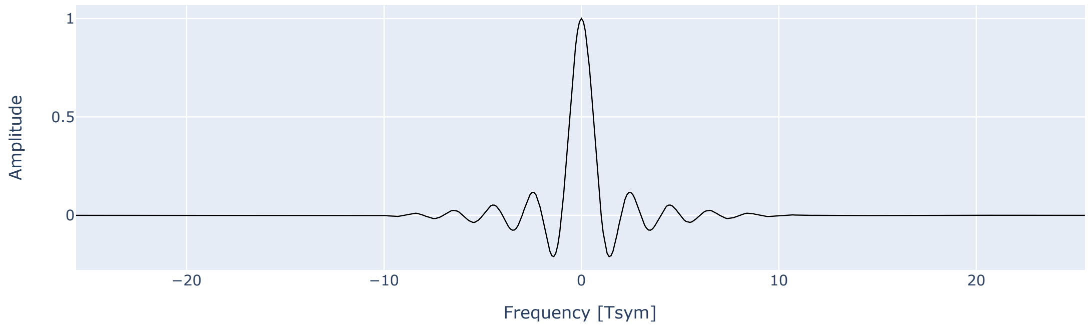

Figure 3.1: Section of Cosine FIR with a resolution of 1024

The signal is now in a appropriate state for the use inside an localization algorithm, where the delays of the signals can be detected by the help of cross-correlation techniques.

$$x_{tSigTB}[k] = Re\{x_{tSigBB}[k] \cdot e^{-2\pi j f_c k}\} \tag{3.2}$$

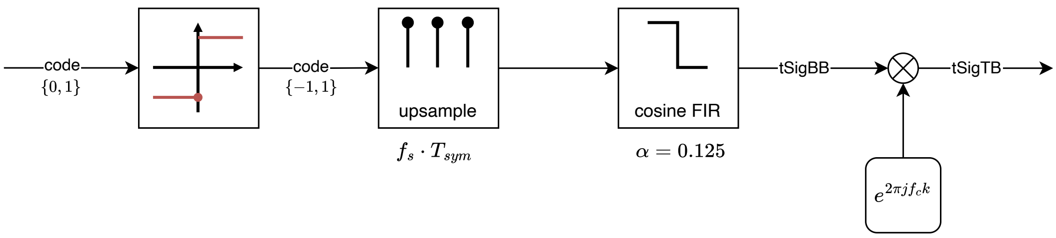

Figure 3.2: Processing of generated signal

3.3 Band pass filter

On the receiver side all signals are received as a sum, which is mixed by artifacts of signal reflections and random noise from the electronics.

The received signal may have noise around its bandwidth. Thus, we only pass though frequencies inside our frequency band by applying a butterworth band pass filter. A flat magnitude is favorable because only frequencies of the base-band should be passed through. The filter gets applied after shifting back to the base-band. Such a filter, namely a maximally flat magnitude filter, approximates this goal. The roll-off decreases by increasing the order of the system.

The critical frequencies of the applied filter are $f_c \pm \frac{bw}{2}$ by an Order of 5. Thus frequencies get removed which are not inside the spectrum of interest. To remove shifts in time the filter is applied forwards and backwards following a doubling of its order. By using the filter twice the order gets doubled.

3.4 Shift to base band

Shifting the transmitted signal back to its original frequency is feasible by just changing its sign. In this case also the imaginary part can be retained.

$$x_{tSigBB}[k] = x_{tSigTB}[k] \cdot e^{2\pi j f_c k} \tag{3.3}$$

3.5 Low-pass Filter

Because .... The same kind of filter, which was used for pruning the carrier frequencies is used as a low-pass. The same Order and twice filtering principle is used.

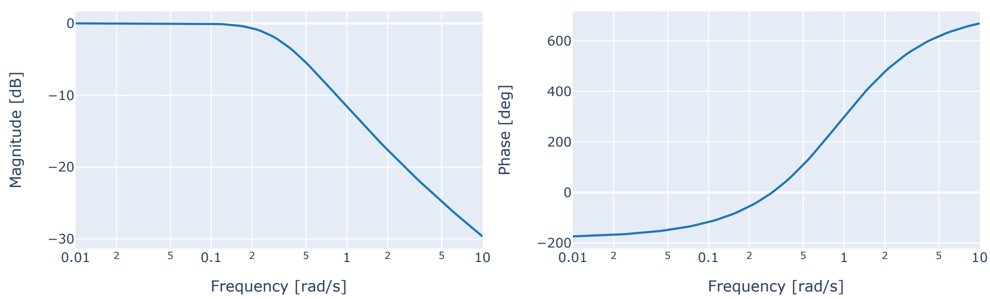

Figure 3.3: Bode plot of 5th order Butterworth low-pass filter

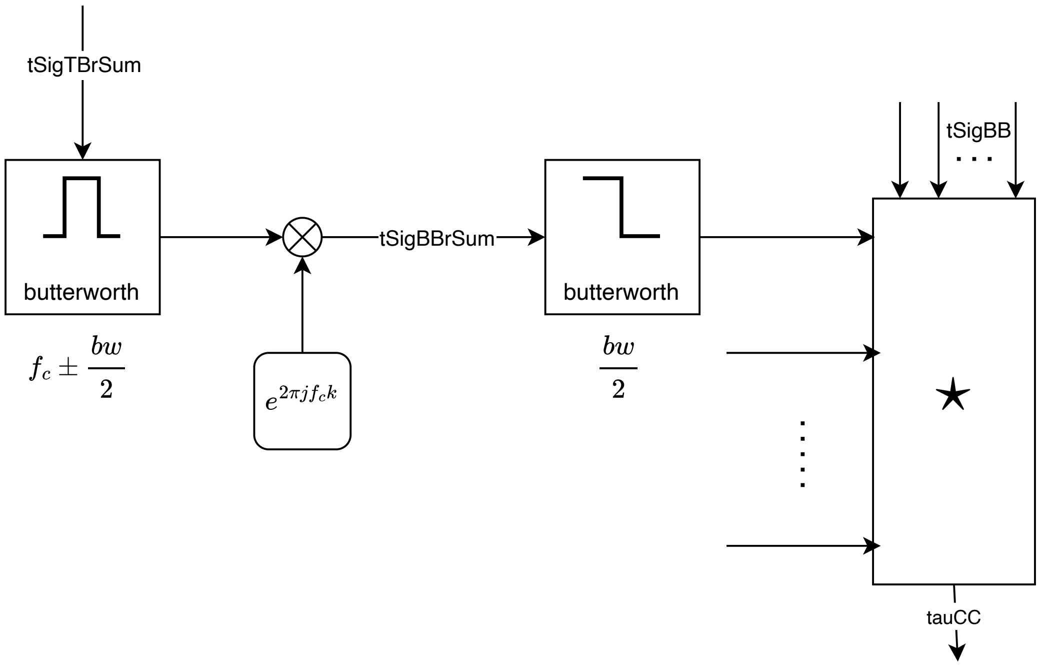

Figure 3.4: Processing of received signal

Chapter 4

Simulation

The simulation consists of a watermark benchmark [vWOJ] and a SNR driven Gaussian white noise added to the sum of the signals.

4.1 Watermark

The Watermark Simulation consists of a convolution or channel replay by an selected channel TVIR estimate. The channels consist of multiple dirac impulses of different strengths. Thus, reflections and reduced signal strength are simulated.

$$x_{tSigTBr}[k] = \sum_{i=0}^{N} h[k,i] \cdot x_{tSigTB}[k-i] \tag{4.1}$$

4.2 White Noise

A additive Gaussian White Noise (GWN) generated by a desired Signal to Noise Ratio (SNR) between $-20dB$ and $20dB$ in steps of $5dB$. From the general equation of the Signal to Noise Ratio we derive our noise standard deviation by transforming this ratio. The white noise is added after the simulation and before receiver filtering. To estimate the power of our signal a standard deviation estimation is used, which consists of all incoming signals by using its expected value. The Gaussian noise is generated by using a normal distributed random variable with its mean at zero and its standard deviation at $\frac{\bar{\sigma}}{SNR}$. Thus, M denotes the number of total anchors and N is the length of the corresponding signal.

$$\bar{\sigma} = \frac{1}{M}\sum_{i=0}^{M} \sigma_i, \quad \sigma_j = \sum_{k=0}^{N} tSigTBr_j{}^2[k] \tag{4.2}$$

$$n[k] = f_{GWN}[k] \cdot \frac{\bar{\sigma}}{SNR}, \quad GWN \sim \text{Normal}(0,1) \tag{4.3}$$

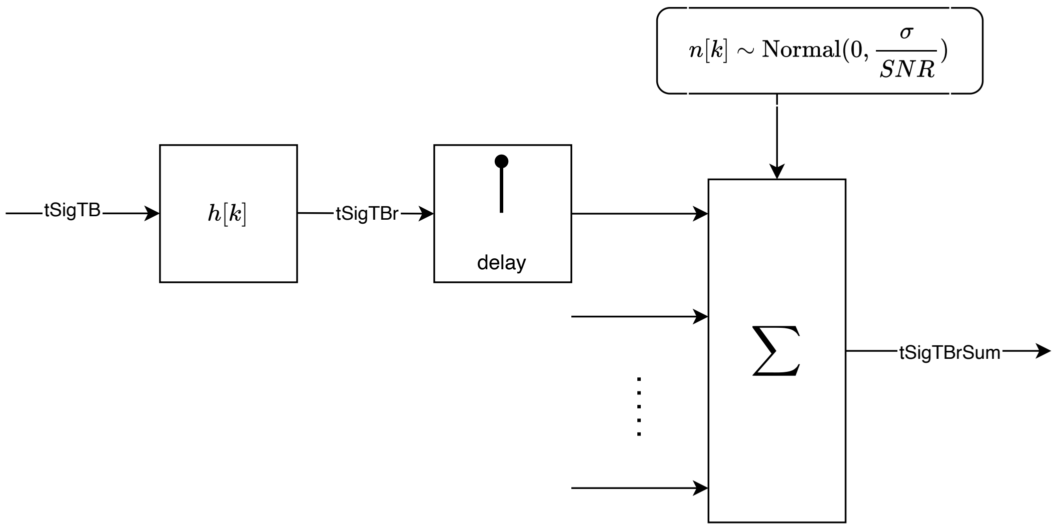

Figure 4.1: Simulation of acoustic signal propagation

Chapter 5

Localization

5.1 Peak detection

The received signal, consisting of summed delayed signals, cross-correlated by every anchor. If the signal is not reflected the peak in cross-correlation would be obvious. But because by the introduction of noise and water reflections a higher rate of similar peaks appear. To suppress these effects a CA-FAR Algorithm [Roh11] is applied to only detect the first reflected peak resulting in lower false alarms of peaks.

CA-FAR works by using multiple values intervals. The most outer one could be described as a train bin and is used to get an estimation of the signals noise. Especially CA-FAR uses averaging to estimate the noise by measured cells. The bordering bin, defined as the guard cells, is used to reduce self-interference of the peaks. Thus, increasing window sizes W results in better noise estimating but overall detectability is still limited by the sample rate [Roh11][rad]. By knowledge of measured peak widths a optimal guard interval can be figured.

The calculated threshold is than scaled by a formula depending on the false alarm rate. The higher the false alarm rate, the weaker high amplitude peaks gets included by the estimated threshold 5.1.

$$T = S \cdot Z, \quad Z_{CA} = \sum_{i=1}^{W} \frac{1}{W} x_{train} \tag{5.1}$$

5.2 Explicit Position calculation

The initial condition for the localization are four anchors S_i with thir coordinates $\{x_i, y_i, z_i\}$ and the target S which is to be located. By multiplying relative delays by the speed of sound c which is approximately set to 1500 $\frac{m}{s}$, the distance d_{ij} between the reference anchor S_0 and S_i is calculated.

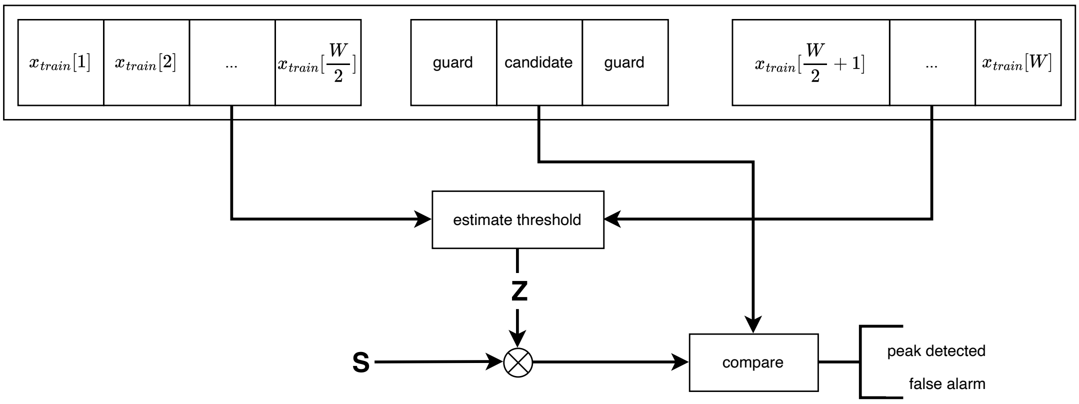

Figure 5.1: CFAR threshold peak detection procedure [Roh11]

$$d_{ij} = c \cdot \tau_{ij} = c \cdot (t_i - t_j), \quad \text{absolute delays } t_k,\ k \in \{0,1,2,3\} \tag{5.2}$$

By these values a Matrix A and vector $\vec{b}$ is created. Thus, a System $A \cdot \vec{x} = \vec{b}$ is established. This linear system can be solved by using the inverse method if Matrix A has full rank. Otherwise least squared can be used but yields undesirable results. In three dimensional Space five anchors are needed for full rank. The solution $\vec{x}$ are the coordinates $\{x, y, z\}$ of the target S [WXX11].

$$A = \begin{bmatrix} x_0 - x_1 & y_0 - y_1 & z_0 - z_1 & d_{01} \\ x_0 - x_2 & y_0 - y_2 & z_0 - z_2 & d_{02} \\ x_0 - x_3 & y_0 - y_3 & z_0 - z_3 & d_{03} \\ x_0 - x_4 & y_0 - y_4 & z_0 - z_4 & d_{04} \end{bmatrix} \tag{5.3}$$

$$\vec{b} = \frac{1}{2} \begin{bmatrix} x_0^2 - x_1^2 + y_0^2 - y_1^2 + z_0^2 - z_1^2 + d_{01}^2 \\ x_0^2 - x_2^2 + y_0^2 - y_2^2 + z_0^2 - z_2^2 + d_{02}^2 \\ x_0^2 - x_3^2 + y_0^2 - y_3^2 + z_0^2 - z_3^2 + d_{03}^2 \\ x_0^2 - x_4^2 + y_0^2 - y_4^2 + z_0^2 - z_4^2 + d_{04}^2 \end{bmatrix}, \quad \vec{x} = \begin{bmatrix} x \\ y \\ z \\ ||S - S_0||_2 \end{bmatrix} \tag{5.4}$$

Theoretically an system A of lower rank can be solve by least squares. Having said this, positions calculated by that approach could not satisfy the demands of 3D localization.

$$\vec{x} = (A^T A)^{-1} A^T \vec{b} \tag{5.5}$$

5.3 GPS like localization method

Because of restrictions introduced in the the first localization method an alternative localization procedure is probed. Thus a position calculation by four anchors is alternatively pursued.

$$x_{ji} := x_j - x_i, \quad y_{ji} := y_j - y_i, \quad z_{ji} := z_j - z_i \tag{5.6}$$

By rearranging the derivation of hyperbola intersections the following substitutes can be defined.

$$\mathbf{A} = \frac{d_{02}x_{10} - d_{01}x_{20}}{d_{01}y_{20} - d_{02}y_{10}}, \quad \mathbf{B} = \frac{d_{02}z_{10} - d_{01}z_{20}}{d_{01}y_{20} - d_{02}y_{10}} \tag{5.7}$$

$$\mathbf{C} = \frac{d_{02}\left(d_{01}^2 + x_0^2 - x_1^2 + y_0^2 - y_1^2 + z_0^2 - z_1^2\right) - d_{01}\left(d_{02}^2 + x_0^2 - x_2^2 + y_0^2 - y_2^2 + z_0^2 - z_2^2\right)}{2\left(d_{01}y_{20} - d_{02}y_{10}\right)} \tag{5.8}$$

$$\mathbf{D} = \frac{d_{23}x_{12} - d_{21}x_{32}}{d_{21}y_{32} - d_{23}y_{12}}, \quad \mathbf{E} = \frac{d_{23}z_{12} - d_{21}z_{32}}{d_{21}y_{32} - d_{23}y_{12}} \tag{5.9}$$

$$\mathbf{F} = \frac{d_{23}\left(d_{21}^2 + x_1^2 - x_1^2 + y_1^2 - y_1^2 + z_0^2 - z_1^2\right) - d_{21}\left(d_{23}^2 + x_1^2 - x_2^2 + y_1^2 - y_2^2 + z_1^2 - z_2^2\right)}{2\left(d_{21}y_{32} - d_{23}y_{12}\right)} \tag{5.10}$$

$$\mathbf{G} = \frac{\mathbf{E} - \mathbf{B}}{\mathbf{A} - \mathbf{D}}, \quad \mathbf{H} = \frac{\mathbf{F} - \mathbf{C}}{\mathbf{A} - \mathbf{D}}, \quad \mathbf{I} = \mathbf{A} \cdot \mathbf{G} + \mathbf{B}, \quad \mathbf{J} = \mathbf{A} \cdot \mathbf{H} + \mathbf{C} \tag{5.11}$$

$$\mathbf{K} = d_{02}^2 + x_0^2 - x_2^2 + y_0^2 - y_2^2 + z_0^2 - z_2^2 + 2x_{20}\mathbf{H} + 2y_{20}\mathbf{J} \tag{5.12}$$

$$\mathbf{L} = 2\left(x_{20}\mathbf{G} + y_{20}\mathbf{I} + z_{20}\right) \tag{5.13}$$

$$\mathbf{M} = 4d_{02}^2\left(\mathbf{G}^2 + \mathbf{I}^2 + 1\right) - \mathbf{L}^2 \tag{5.14}$$

$$\mathbf{N} = 8d_{02}^2\left[\mathbf{G}\left(x_0 - \mathbf{H}\right) + \mathbf{I}\left(y_0 - \mathbf{J}\right) + z_0\right] + 2\mathbf{L} \cdot \mathbf{K} \tag{5.15}$$

$$\mathbf{O} = 4d_{02}^2\left[\left(x_0 - \mathbf{H}\right)^2 + \left(y_0 - \mathbf{J}\right)^2 + z_0^2\right] - \mathbf{K}^2 \tag{5.16}$$

A downside of this approach is the uncertainty of position z. Thus, additional information on bounds is necessary. The target won't get above sea level. Consequently, at least one boundary $z_{surface}$ which acts like a maximum can be set. The minimum value z_{ground} can be assumed as the lowest position achievable underwater.

$$z_{a,b} = \frac{\mathbf{N}}{2\mathbf{M}} \pm \sqrt{\left(\frac{\mathbf{N}}{2\mathbf{M}}\right)^2 - \frac{\mathbf{O}}{\mathbf{M}}} \tag{5.17}$$

$$z = \min\left\{\max\left\{z_a,\ z_b,\ z_{surface}\right\},\ z_{ground}\right\} \tag{5.18}$$

The resulting x and y values of our target can then be calculated by the following formula using the selected z.

$$\vec{x} = \begin{bmatrix} x \\ y \\ z \end{bmatrix} = \begin{bmatrix} \mathbf{G}z + \mathbf{J} \\ \mathbf{I}z + \mathbf{H} \\ z \end{bmatrix} \tag{5.19}$$

Bibliography

[Gen07] Ken Gentile. Digital pulse-shaping filter basics, 2007.

[GK65] R. Gold and E. Kopitzke. Study of correlation properties of binary sequences. *Interim Tech. Rep.*, 1–4(1), 1965.

[MD] Steven J. Merrifield and John C. Devlin. The implementation of a multiplexing gold codegenerator using a xilinx logic cell array. *School of Electronic Engineering, La Trobe University*.

[PPWW72] William Wesley Peterson, Wesley Peterson, Edward J Weldon, and Edward J Weldon. *Error-correcting codes*. MIT press, 1972.

[PS08] John G. Proakis and Masoud Salehi. *Digital Communications*. McGraw-Hill Higher Education, New York, 2008.

[rad] Falschalarmrate - radar basics. https://www.radartutorial.eu/01.basics/Falschalarmrate.de.html. Accessed: 2022-11-08.

[Roh11] Hermann Rohling. Ordered statistic cfar technique - an overview. In *2011 12th International Radar Symposium (IRS)*, pages 631–638, 2011.

[SP80] Dilip V Sarwate and Michael B Pursley. Crosscorrelation properties of pseudorandom and related sequences. *Proceedings of the IEEE*, 68(5):593–619, 1980.

[vWOJ] Paul van Walree, Roald Otnes, and Trond Jenserud. Watermark.

[WXX11] Yang Weng, Wendong Xiao, and Lihua Xie. Total least squares method for robust source localization in sensor networks using tdoa measurements. *International Journal of Distributed Sensor Networks*, 7(1):172–902, 2011.

Appendix A

Content of the DVD

In this chapter, you should explain the content of your DVD.